# Vitreous deformation during eye movement

Piccirelli, Marco ; Bergamin, Oliver ; Landau, Klara ; Boesiger, Peter ; Luechinger, Roger

Abstract: Retinal detachment results in visual loss and requires surgical treatment. The risk of retinal detachment depends, among other factors, on the vitreous rheology, which varies with age. To date, the viscoelasticity of the vitreous body has only been measured in cadaver eyes. However, the ex vivo and in vivo viscoelasticity may differ as a result of the effect of intravitreal membranes. Therefore, an MRI method and appropriate postprocessing tools were developed to determine the vitreous deformation and viscoelastic properties in the eyes of living humans. Nineteen subjects (eight women and 11 men; mean age, 33 years; age range, 14-62 years) gazed at a horizontal sinusoidal moving target during the segmented acquisition of complementary spatial modulation of magnetization images. The center of the lens and the scleral insertion of the optic nerve defined the imaging plane. The vitreous deformation was tracked with a dedicated algorithm and fitted with the commonly used viscoelastic model to determine the model parameters: the modified Womersley number a and the phase angle b. The vitreous deformation was successfully quantified in all 17 volunteers having a monophasic vitreous. The mean and standard deviation of the model parameters were determined to be 5.5 $\pm$ 1.3 for a and -2.3 $\pm$ 0.2 for b. The correlation coefficient (-0.76) between a and b was significant. At the eye movement frequency used, the mean storage and loss moduli of the vitreous were around 3 $\pm$ 1 hPa. For two subjects, the vitreous deformation was clearly polyphasic: some compartments of the vitreous were gel-like and others were liquefied. The borders of these compartments corresponded to reported intravitreal membrane patterns. Thus, the deformation of the vitreous can now be determined in situ, leaving the structure of the intravitreal membranes intact. Their effect on vitreous dynamics challenges actual vitreous viscoelastic models. The determination of the vitreous deformation will aid in the quantification of local vitreous stresses and their correlation with retinal detachment.

DOI: https://doi.org/10.1002/nbm.1713

Full title of the paper:

Vitreous Deformation during Eye Movement

Short title of up to 70 characters:

Vitreous Deformation during Eye Movement

Names and affiliations of all authors.

Marco Piccirelli [1,2,3], Oliver Bergamin [3], Klara Landau [3], Peter Boesiger [2], Roger Luechinger [2]

[1] Branco-Weiss Laboratory for Social and Neural Systems Research, Empirical Research in Economics, University of Zurich, Zurich, Switzerland

[2] Institute for Biomedical Engineering, University and ETH Zurich, Zurich, Switzerland

[3] Department of Ophthalmology, University Hospital Zurich, Zurich, Switzerland

Give the full address, including e-mail, telephone and fax, of the author who is to check the proofs.

Marco Piccirelli

UniversitätsSpital Zürich / SNS-Lab

Postfach 146

Rämistr. 100

8091 Zürich/CH

pmarco@ethz.ch

phone: +41 44 255 4493

Sponsors of the research contained in the paper:

Swiss National Science Foundation (SNF #3100AO-102197)

Technical and financial support of Philips Healthcare, Best, NL

## Graphical Abstract:

Full title of the paper:

Vitreous Deformation during Eye Movement

Names of the authors:

Marco Piccirelli, Oliver Bergamin, Klara Landau, Peter Boesiger, Roger Luechinger

Short abstract of not more than 80 words or 3 sentences of text summarising the key findings presented in the paper:

Vitreous deformation during eye movement was depicted using tagging and tracked with a dedicated algorithm. Inhomogeneous deformations' pattern and viscoelastic properties could be revealed inside the vitreous . The viscosity and elasticity of the vitreous was quantified in-vivo from its deformation with an analytical model, and the results are depicted here as a function of subject age.

Figure:

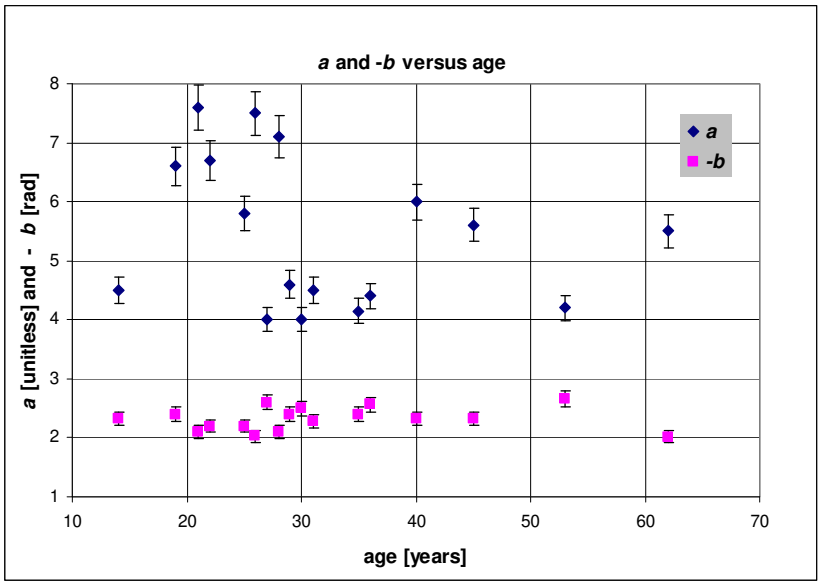

# *Vitreous Deformation during Eye Movement*


# Abstract

Retinal detachment results in visual loss and requires surgical treatment. The risk of retinal detachment depends, among other factors, upon the vitreous rheology, which varies with age. Up to now, the viscoelasticity of the vitreous body has only been measured in cadaver eyes. However, the ex-vivo and in-vivo viscoelasticity may differ, due to the effect of intravitreal membranes. Therefore, a MRI method and appropriate postprocessing tools were developed to determine the vitreous deformation and viscoelastic properties in eyes of living humans. Nineteen subjects (8 women and 11 men; mean age: 33 years; age range: 14 to 62 years) gazed at a horizontal sinusoidal moving target during the segmented acquisition of CSPAMM images. The center of the lens and the scleral insertion of the optic nerve defined the imaging plane. The vitreous deformation was tracked with a dedicated algorithm, and fitted with the commonly used viscoelastic model to determine the model parameters: the modified Womersley number *a* and the phase angle *b*. The vitreous deformation was successfully quantified in all 17 volunteers having a monophasic vitreous. The model parameters' mean and standard deviation were determined to be 5.5±1.3 for *a* and -2.3±0.2 for *b*. The correlation coefficient (-0.76) between *a* and *b* is significant. At the eye movement frequency used, the mean storage and loss moduli of vitreous are around 3±1 hPa. For two subjects, the vitreous deformation is clearly polyphasic: some compartments of the vitreous are gel-like and others liquefied. These compartments' boarders correspond to reported intravitreal membrane patterns. The deformation of the vitreous can now be determined in situ, leaving the structure of the intravitreal membranes intact. Their effect on vitreous dynamics, presumably, challenges actual vitreous viscoelastic models. The determination of the vitreous deformation will help quantify local vitreous stresses and their correlation with retinal detachment.


**Keywords:** tagging, tracking algorithm, vitreous, viscosity, elasticity, retinal detachment

**Abbreviations:**

| | |
|---|---|
| CSPAMM | Complementary SPAtial Modulation of Magnetization |
| EPI | Echo Planar Imaging |
| HARP | HARmonic Phase |

# Introduction

The vitreous is a viscous aqueous solution structured by collagen fibers and hyaluronic acid polymers.(1,2) It fills the intraocular space between the lens and the retina. The primary role of the vitreous is to maintain the ocular globe volume, and therefore it needs to be replaced after vitrectomy. Nevertheless, the vitreous and its potential substitutes have to fulfill several other functional and physiological constraints,(3) the most obvious being transparence to visual light and adequate refraction index. To maintain good vision, appropriate osmotic pressure and viscoelastic properties are important as well.(4)

The vitreous viscoelasticity has both a biochemical and a mechanical impact on the retina. First, it influences diffusive and convective molecular transport.(5) The transport of oxygen and cytokines through the vitreous modifies retinal angiogenesis. Retinal neovascularization can induce traction retinal detachment.(3) Second, the vitreous viscoelasticity has an impact on the shear stress induced by the vitreous on the retina during eye movement. Excessive shear stress can damage the retina and - once a retinal tear develops – will induce filling of the subretinal space with liquefied vitreous, which separates the photoreceptors from the underlying retinal pigment epithelium, leading to retinal detachment that requires surgical treatment in order to prevent permanent visual loss.(3,6)

Collagen membranes compartmentalize the vitreous space. In each of these compartments, the vitreous viscoelastic properties may vary. The binding between these collagen membranes with the hyaluronic acid polymers also impacts on the viscoelastic properties of the vitreous.(2,7) Moreover, the connections of these membranes (going through the retina) with the sclera impede the vitreous deformation locally and increase the (shear) stress acting on the retina, thus increasing the risk of retinal detachment.

The movement of the vitreous relative to the retina is easily revealed by the movement of floaters when moving the eye.(8) Nevertheless, so far, the viscoelasticity of the vitreous body has been measured only ex-vivo,(7) where it varied as a function of the location inside the eyeball.(9) In-vivo vitreous deformation data are limited to the work of Zimmerman in 1980, who measured optically the relaxation pattern of the vitreous after a step rotation (saccade) of the eye,(10) and Walton et al. in 2002, who used ultrasound.(11) Applying these methods, only the bulk movement of the whole vitreous was considered, so inhomogeneous deformation within the vitreous could not be observed. Buchsbaum, et al. in 1984 tested the adequacy between the vitreous viscoelasticity data obtained ex-vivo and the Zimmermann's in-vivo relaxation pattern.(12) The concordance was found to be poor, according to Buchsbaum (p. 294), due to the excessive eye accelerations used by Zimmermann and to a potential inhomogeneity of the vitreous viscoelastic properties, among other factors.

A sinusoidally moving gaze target induces the most accurate eye movements. Vitreous deformation during sinusoidal eye movement has been modeled as a spherical homogenous fluid rotating around a diameter.(12,13) This analytical model uses two dimensionless parameters *a* (modified Womersley number) and *b* (phase angle),

$$a = R_0\sqrt{\omega/|\varepsilon + i\nu|} \qquad \text{and} \qquad b = \arctan\left(-\nu/\varepsilon\right),$$

from which the kinematic viscosity $\nu$ and elasticity $\varepsilon$ can be derived:

$$\varepsilon = \frac{\omega R_0^2}{a^2\sqrt{1+\tan^2 b}} \qquad \text{and} \qquad \nu = -\varepsilon\tan b\,,$$

where $R_0$ represents the eye radius and $\omega$ the circular frequency. The relation to the complex shear modulus $G$ is:

$$G = G' + iG'' = \rho\omega\left(\varepsilon + i\nu\right),$$

where $\rho$ is the mass density and $G'$ and $G''$ are the elastic and viscous components of the modulus, respectively. This model is based on the assumption that the viscoelastic properties are homogeneous throughout the vitreous. David et al. in 1998 used ex-vivo vitreous viscoelasticity(9) to describe the vitreous deformation.(13) To better understand the vitreous deformation pattern and to validate

simulations,(12-14) eyeball models have been built.(15,16) Hardware models were needed, as no in-vivo measurements methodology existed.(17) However, these models can neither take into account the complex structure of the vitreous(1) nor the inter-subjects differences in vitreous properties.

Attempts to determine the mechanical properties of orbital tissues in-vivo have been done using MR Elastography.(18,19) MR Elastography encodes the propagation of externally induced shear waves with phase-locked bipolar gradients.(20) MR Elastography of the vitreous delivers good results post-mortem(21) or under anesthesia in animal models(22). Nevertheless, MR Elastography encoding is degraded in-vivo by the small eye movements necessary to maintain fixation.(23) Even at a resolution of 0.2x0.2 x1.0$mm^3$ conventional MRI(24) could not provide the desired breakthrough in the understanding of the intrinsic vitreous structure.(17,25)

To clarify the role played by the intravitreal membranes, using – instead of antagonizing – eye movements, a MRI method phase-locked to the eye movement itself was developed to determine the vitreous deformation and estimate the viscoelasticity in-vivo. The local deformation of the vitreous during sinusoidal eye movements was visualized and quantified. Specific postprocessing software was developed to track the deformation of the monophasic vitreous through the entire ocular movement. The applicability of the commonly used analytical model first described by Buchsbaum et al.(12-14) to estimate the viscoelastic properties of the vitreous in-vivo will be discussed. The change of the vitreous viscosity with age was investigated, as the vitreous is commonly assumed to liquefy with age.(23)

# Materials and Methods

## Subjects and Setup

The study was conducted according to the tenets of the Declaration of Helsinki and approved by the ethics committee of the Health Department of the Canton of Zurich, Switzerland. Each subject agreed to participate after the scientific value and possible risks of the study were explained. The right eye of

nineteen healthy subjects (eight women and eleven men; mean age: 32 years; range: 14 to 62 years of age) were imaged. Visual acuity of all subjects was sufficient to track the visual stimulus.

A horizontal oscillating white square on a black background (target size = 0.4°, luminance = 5.1 ± 1 cd/mm$^2$ on a background of 0.05 ± 0.02 cd/mm$^2$) was used to induce sinusoidal smooth pursuit eye movements with an amplitude of ±20° and a period of 2s (corresponding to a maximal angular eye velocity of 63°/s). Sinusoidal movements were chosen because the vitreous model used to fit the imaged deformation is analytically solvable for sinusoidal eye movements. For the presentation of the visual stimulus, a computer, projector, projection screen, and the software "Presentation" (Neurobehavioral Systems Inc., Albany CA, USA) were used as described in Piccirelli et al.(26) A mirror allowed the subjects to gaze out of the bore to the projection screen. For the MR signal acquisition, a receive-only surface coil of 47mm diameter was placed on the right eye like a monocle, so that the subject could see the target through it. Foam pads immobilized the subject's head. The room light was turned off to maximize the contrast of the stimulus.

## MRI Sequence

Axial 2D CSPAMM (Complementary SPAtial Modulation of Magnetization) tagging images(27) were acquired on a 1.5T MRI scanner (Achieva 1.5T; Philips Healthcare, Best, The Netherlands) with a multishot segmented echo planar imaging (EPI) gradient echo sequence (Figures 1 and 2). The lens center and the scleral insertion of the optic nerve defined the imaging plane. The 40° right-to-left eye movement was split into fifteen time frames of 70ms (with 12ms of acquisition and 58 ms of separation), resulting in a total acquisition of 15x70=1050ms. The remaining 950ms of the 2s periodic eye movement served for MR signal recovery. The tagline distance was 3mm. Other parameters were identical to those described previously: 140 × 140 mm$^2$ field of view, 1.2 × 1.2 × 4.0 mm$^3$ scan resolution, 8 signal averages, and a 256 × 256 reconstruction matrix.(26) The use of an EPI factor of 5 shortened the acquisition time to 4.5 minutes.

** Insert Figure 1 and Figure 2 about here **\

## Postprocessing

A postprocessing technique specially dedicated to the vitreous geometry was developed, based on the mesh tracking algorithm introduced by Piccirelli, et al.(28)

The vitreous was overlaid at the 9$^{th}$ timeframe (approximately gaze straight ahead) with a 60x36 radial mesh centered on the center of rotation and with its outermost polygon on the sclera (in green in Fig3, middle Panel). To ascertain that the meshes lay only on the vitreous, we took anatomical images as references and realigned the meshes if needed.

** Insert Figure 3 about here **\

Using the dedicated mesh-algorithm, the mesh vertices were tracked through 15 time frames. The software was based on TagTrack 1.7.0 (GyroTools Ltd., Zurich, Switzerland) integrating HARmonic Phase (HARP)(29) with peak-combination.(30) A circular band pass filter was applied to extract the harmonic peak in Fourier space. The diameter of the filter corresponded to 2.3 image pixels.(31)

The quantified vitreous deformation could be used to challenge the analytical model commonly used to describe the vitreous deformation.(12-14) As opposed to the data obtained by Zimmermann during fast eye movements,(10) the deformation of the vitreous during rather slow sinusoidal eye movement should be better described by the model. In effect, the model estimates the vitreous deformation for repetitive sinusoidal eye movements. If this model correctly describes the physics of the vitreous deformation, then the viscoelastic properties of the vitreous can be estimated by fitting the model parameters to the observed vitreous deformation.

The rotation angle of each concentric polygon forming the mesh was used to find the parameters *a* and *b* – of the analytical model described in Buchsbaum et al.(12) – best describing the vitreous motion. A L2 norm showed the best fitting results. To avoid fitting problems, if several of the outermost polygons exhibited a similar rotation pattern (difference<0.5°) at the interface vitreous-sclera, only the innermost of these polygons were considered to lay on the interface sclera-vitreous (or vitreous cortex-vitreous center) and were included in the fitting procedure. By doing so, polygons lying on the sclera that would

spoil the fitting of the model were avoided, which assumes that only the outermost polygon is lying on the interface sclera-vitreous. The radii of the outermost and innermost polygons were taken into account for fitting. The outermost polygon rotation amplitude was determined and included in the model, before the rotation of the concentric polygons as a function of time was fitted with the analytic viscoelastic model(12,13) to determine the parameters *a* and *b*. The fit was done for *a* in the range [1:20] with a step of 0.19, and for *b* in the range [–3.0:–0.1] with a step of 0.03. Nota bene, a mechanical system at a movement frequency higher than a (potential) resonance frequency, will have a phase shift below -π/2,(32) which implies that the value of *b* would be $-\pi < b < -\pi/2$, even for an overdamped system. This impacts the sign of the viscosity, but not the elasticity, as seen from the above equations.

To verify the consistency and stability of the post-processing procedure, the accordance of the mesh rotation between several datasets (acquired on the same day) was checked for each subject. In addition, for four subjects, the left-to-right eye movement was acquired. Finally, for the same four subjects, the whole procedure was repeated on another day.

** Insert Figure 4 about here **\

# Results

For all 19 subjects, the acquisition of CSPAMM images of the vitreous deformation was successful. The reproducibility of the final fitting results for acquisitions on two different days and eye movement directions were, for the first four subjects, within a 10% range, i.e. the obtained values *a* and *b* did not vary by more than 10%. Therefore only one examination with one movement direction (adduction) was acquired for the 15 following subjects.

The vitreous deformations of two subjects (women, 51 and. 22 years old) were clearly polyphasic, i.e. divided into compartments of different viscoelastic properties. During eye movement, some compartments of the vitreous underwent only bulk deformation, i.e. did not or only slightly deform, whereas others underwent swirling deformations (Fig1, subjects 2 and 3). These compartments seemed

sharply separated (doted red lines in Fig1), corresponding to reported intravitreal membrane patterns.(1,33,34) For subject 2, the posterior part of the vitreous remained almost static and deformed only slightly. On the contrary, the anterior part was affected by the eye movement and deformed more strongly. Subject 3's vitreous showed a complex compartmental structure. Four vitreous compartments with different deformation patterns could be differentiated. These compartments are oriented perpendicularly to those of subject 2.

The other 17 subjects had a monophasic vitreous (i.e., homogeneous viscoelasticity), with a deformation pattern similar to subject 1 (Fig1) and Fig2. The vitreous exhibited concentric deformation movements around a rotation center. The phase and the amplitude of these concentric rotations depended upon their distance to the rotation center and were subject dependent. With increasing distance from the rotation center, the vitreous rotation amplitude increased and the phase shift relative to the eye movement decreased. The deformation of the vitreous was reversible, and after a period of the movement came back to the original configuration, as expected for laminar flows.

Quantitative evaluation could be obtained for all 17 subjects with a monophasic vitreous, as the vitreous deformation could be successfully tracked over the whole movement range, using the dedicated mesh algorithm (Fig3). Each of the concentric polygons could be tracked through the 15 time frames. Nevertheless, some inconsistency of the mesh due to tracking imperfection was still visible in the locations of the highest shear deformation. For subject 1, the four outermost polygons described the same rotation patterns, and therefore were considered to lay on the sclera. The rotations of the inner 32 concentric polygons were plotted in function of time in Fig4A (for the mesh of Fig3). The outermost polygon underwent a sinusoidal rotation slightly below 40°, in concordance to the gaze movement. The rotation of the other polygons differed in amplitude and phase. The innermost polygon changed its rotation direction around 0.3s after the sclera, had a movement range of nearly 16° and a phase delay relative to the sclera of nearly 1.3s. As expected for a viscoelastic fluid, the amplitude and phase varied smoothly from the innermost to the outermost polygon.

By fitting the vitreous deformation with the analytical model, the parameters *a* and *b* could be specifically determined (Fig4B). For comparison, the deformation pattern expected from ex-vivo vitreous viscoelasticity measurements is depicted in Fig4D. This procedure was repeated for all 17 subjects with a monophasic vitreous. The *a* and *b* values are plotted in function of the subject's age (Fig5). The values obtained for *a* vary from 4.0 to 7.6, and for *b* from – 2.66 to –2.02. The correlation coefficients between the age and *a* respectively *b* are -0.27 and 0.09 - both not significant. The correlation coefficient between *a* and *b* is -0.76 - significant with a double-sided p-value smaller than 0.01.

** Insert Figure 5 about here **\

# Discussion

The deformation of the vitreous during sinusoidal eye movement was determined in-situ, revealing the topology of the intravitreal structures' influence on the vitreous dynamic. Polyphasic and monophasic vitreous could be differentiated. For the first time, the inhomogeneous deformation of the monophasic vitreous could be quantified in vivo. These results challenge the commonly used viscoelastic deformation model of the vitreous, and the assumed deformation pattern and the resonance properties of the system, and accentuate the need for extended models.

The presented method resolves the local deformation of the vitreous during eye movement. In the image plane, the local movement of the vitreous can be followed up to the scale of the image resolution. The combined use of HARP(29) (to downsize the smallest displacement resolvable) and of sequential acquisition (to shorten the time phase duration) made the determination of the vitreous viscoelasticity possible, as discussed by Buchsbaum.(12) Inhomogeneous deformation patterns inside the vitreous can be determined for both monophasic and polyphasic vitreous. The good signal to noise ratio (SNR) of the vitreous tagging pattern was achieved due to the use of a small surface coil, and to the long MR signal recovery time of the vitreous.(27)

## Determination of the Vitreous Deformation in-vivo

For a monophasic vitreous, the rotation angle as a function of the distance to the rotation center was resolved and quantified. By contrast, the movement of "mouches volantes" gives only a basic impression of the vitreous deformation,(8) that lacks systematic description of the vitreous deformation. Zimmermann, in 1980, was the first to investigate quantitatively the vitreous deformation during eye movement.(10) With an optical system, the relaxation of the vitreous after saccadic eye movements was determined. A laser beam traversing the vitreous was used to depict a scattering pattern on the retina. The movement of this scattering pattern was used to describe the vitreous deformation. This method assumes the vitreous rotates as a single bulk solid, and therefore a single angle was defined to describe the vitreous rotation over time. Zimmerman's method's major drawback is the exclusion of shear deformations of the vitreous. The same concerns apply to ultrasound methods.(11) The smaller rotation angle of the inner vitreous compared to the outermost vitreous is presumably due to dissipation of the traction force acting on the vitreous periphery.

The reversibility of the vitreous deformation during the second half of the movement was easily tested. To visualize the deformation of the vitreous over the whole period (right-to-left and left-to-right) of the eye movement, 32 time frames (instead of 15) were acquired for some subjects with monophasic vitreous(see Fig2), and so we took advantage of the long MR signal recovery time of the vitreous magnetization ($T_1$~5s).(35) The deformation of the vitreous was reversible, indicating that only a small amount of dissipative turbulent flow was created during the movement. Analytical simulations(14) and hardware models(16) predicted turbulent flow in the neighborhood of the eye lens. The presence of intravitreal membranes(34) may be responsible for diminishing the turbulences around the lens. Only at the vitreous-sclera interface was a small signal decrease observed. This could be due to magnetic field inhomogeneities or to the $T_1$ difference between the retina and the vitreous.

The image resolution was sufficient to resolve regions of different deformation patterns inside the vitreous. The viscoelastic deformation varied between subjects. For the 17 subjects with monophasic vitreous, the qualitative comparison between the depth and the phase shift of the peripheral movement

propagation into the center of the vitreous allows a rough estimation of the underlying viscoelastic vitreous properties. Moreover, for the first time the convection of the vitreous predicted by a vitreous membrane model(36) was observed.

Two of the 19 studied subjects had a polyphasic vitreous and their deformation patterns were very different from each other. The vitreous of subject 2 (woman, 51 years old, low myopia) was separated in two zones (Fig1). The anterior zone deformed more than the posterior zone. This anterior-posterior separation could be due to vitreous collapse(23,37) or to inhomogeneities of the vitreous structure(33). Vitreous collapse is a common aging process,(38) as 65% of the population older than 65 years have a detached vitreous.(23) During shrinkage, the vitreous detaches from the posterior retina and fluid vitreous humor fills the space between the collapsed vitreous structure and the retina. This process may occasionally lead to the development of peripheral retinal tears at the site of the anteriorly located vitreous base and ultimately to retinal detachment. The deformation of the anterior part of subject 2's vitreous during the eye movement may be due to the presence of fibers connecting the retina with the vitreous and to the resulting higher vitreous viscosity. On the contrary, in the less viscous posterior vitreous, where the collagen fibers are absent after a collapse, only little vitreous deformation is visible.

In contradistinction, the zone pattern of subject 3's vitreous (woman, 22 years old, high myopia) does not correspond to a vitreous collapse pattern. The four observed zones are oriented in the anterior-posterior direction. This orientation is rather consistent with an intact vitreous structure, as reported by Eisner.(34,37) The two compartments on the medial and lateral side of the vitreous especially seem to correspond to the reported tractus preretinalis originating at the ora serrata.(1) Nevertheless, the alternation of zones of different viscoelasticity does not correspond to Worst's description of a more rigid vitreous cortex and a more fluid inner core.(1)

## Quantification of the Vitreous Deformation and Vitreous Viscoelastic Model

The quantification of the vitreous deformation challenges the commonly used viscoelastic vitreous deformation model.(12-14) This model assumes small displacement amplitudes. Our main finding is that

the in vivo viscoelastic deformation of the vitreous can be satisfyingly fitted by this simple analytical model only for values of the parameter *b* lower than -π/2. The phase shift of the rotation of the inner vitreous relative to the sclera was bigger than π/2; i.e. $-\pi < b < -\pi/2$. Therefore the mechanical system studied has a resonance frequency which is lower than the one used for the eye movements (0.5Hz).

The parameter *a* (modified Womersley number) decreases with age (see Fig5). Nevertheless, the correlation between age and *a* is rather weak (-0.27). The correlation coefficient between *a* and *b* is relatively high: -0.76. From the obtained *a* and *b* values, the viscosity and elasticity are derived as summarized in Table 1:

** Insert Table 1 about here **\

The viscoelastic deformation determined in-vivo differs remarkably from the one expected by the simple analytical model using averaged ex-vivo viscoelasticity measurements. As mentioned by Nickerson et al.,(7) this difference might be explained by the degradation of the intravitreal collagen fiber structure through the vitreous extraction,(9) the time elapsed between the extraction and the ex-vivo measurements, or several others issues related to ex-vivo viscosity measurements.(39) A modification of the hyaluronic acid polymerization state could also impact on the vitreous viscoelastic properties.(1) Even after age related vitreous liquefaction, collagen structures, eventually collapsed, are still present inside the eye globe, and can affect the vitreous rheology. Moreover, the variety of methodologies, shear frequencies, and viscosity definitions used in the literature(7,9,12,40-42) combined with frequency dependence and bimodality(43) of the vitreous viscoelasticity, make a meaningful comparison difficult. Nevertheless, the value found for the storage and loss components of the viscoelastic modulus G - at the relatively low eye movement frequency used - are around 3±1 hPa, which is one order of magnitude above the values obtained from the high frequency ex vivo measurement made after degradation of the intravitreal membranes.(7,12,40)

The viscosity and the elasticity act both on the depth and on the phase shift of the propagation of the sclera movement into the center of a monophasic vitreous. Nevertheless, the propagation depth and

phase shift are the relevant mechanical properties of the movement that determine the local shear stresses inside the eye globe. Therefore, it seems reasonable to postulate that the appropriate description of pathological vitreous will not be its viscoelasticity, but its movement propagation depth and phase shift.

## Main Limitations and Future Developments

The analytical model assumes homogeneous viscoelastic properties of the fluid and a spherical shape of the vitreous space. Furthermore, the model is linear in the force deformation relationship, which may not hold for the relatively big deformation observed. Nevertheless, an “apparent” viscoelasticity of the subjects’ vitreous can be determined. The small difference between 2D and 3D models with a spherical or anatomically correct eye shape, pointed out by Repetto et al., is not relevant for our study.(14,15) The concavity of the vitreous space created by the eye lens has a small but not negligible impact on the deformation pattern. Other models, taking into account the geometry of the eye globe,(15,16) would presumably improve the biomechanical understanding of our in-vivo data. For example, the simple membrane model proposed by Repetto et al. in 2004 (see their Fig7),(36) could explain the observed pattern of vitreous convention, which slightly modified the location of the vitreous whirling center for the right-to-left eye movement compared to the left-to-right eye movement.

For some subjects, several concentric polygons in the periphery described the same rotation over time. A possible explanation could be the rather rigid cortex of the vitreous moving similarly to the sclera to which it is attached. Another explanation could be the limited resolution and the relatively high signal intensity of the sclera at the first time frame, inducing several polygons to describe the rotation pattern of the sclera. The analytical model is not able to take into account varying viscoelastic properties, therefore only the innermost of the polygons describing a rotation similar to the outermost polygon was considered for fitting. Therefore, the effective radius of the innermost polygon was used for fitting.

The limited resolution of the acquired images and the further worsening due to harmonic peak extraction(44) may prevent the visualization and moreover the quantification of the details of vitreous deformation, like the deformation in the neighborhood (< 2mm) of the eye lens. Moreover, due to the

ample vitreous rotation, the limited resolution in conjunction with the quite broad tagline distance creates signal voids through partial volume effects. Vitreous whirling induces the tagging pattern to fade, making the deformation tracking more difficult. The accuracy of the determination of the vitreous rotation center is limited by the resolution and the non-automatic procedure. On the other hand, the limited resolution itself and the size of the innermost polygon give a tolerance upon the exact determination of the rotation center. The ocular lens and intravitreal structures may also modify the position of the whirling center of the vitreous depending upon the eye movement direction, as has been modeled by Repetto et al.(36)

The effect of the HARP filter size on the quantification of the deformation pattern was also tested. In fact, a primary resolution limitation of rotation angle of small structures is inherent to the HARP filtering. The smaller an object is, the broader its Fourier transform. For an object of double the size of the acquired resolution almost no rotation can be depicted without losing information about the object size or shape. For an object of the size of the image, the maximal illustratable rotation is of 60° - using a circular HARP filter. The vitreous was about 2.5cm in diameter. If it rotated as a whole, the maximal illustratable rotation would be of around 55°. From an object of about one fifth of the vitreous size, SNR begins to decrease as soon as the rotation exceeds 30°. As the quantification of the deformation pattern remained unchanged by increasing the filter size, it was concluded that the filter size used was sufficient.

As pointed out by Buchsbaum,(12) the viscoelasticity may depend upon the movement range and speed. Similar experiments with different eye movements may provide further insight into any non-linearities of vitreous mechanical properties.

In conclusion, our novel method enabled us to rigorously validate or refute models of vitreous dynamics in-vivo. The difference between the observed deformation of the vitreous and the one expected from ex-vivo measurements of the vitreous viscoelasticity is remarkable, and is presumably due to the presence of intact intravitreal structures. A model incorporating membranes immerged into a viscoelastic fluid inside an eye ball geometry including the eye lens could probably adequately explain our reported in-vivo data of vitreous deformation.

Noteworthy, and possibly relevant for eye movement control,(45) is the modification of the eye ball inertia through the vitreous deformation. This issue should be considered when modeling the orbital mechanics.

Further studies are needed to investigate if the vitreous viscoelasticity and/or the tractions at the vitreous base are relevant for retinal tears to appear. Saccadic eye movements may give rise to an informative decay phase, especially for the determination of resonance frequencies, as shown by Zimmermann.(46) The vitreous rheology may also play a role in eye lens pathologies. Epidemiological studies about vitreous liquefaction were, up to now, unlikely to be measured.(47) We now provide a tool that makes it possible to approach these clinically relevant topics.

# Acknowledgments

We are thankful to Dr. Gérard Crelier (GyroTools Ltd., Zurich, Switzerland) for providing the TagTrack source code, to Christopher Bockisch for a critical reading of the manuscript, and to the Swiss National Science Foundation (SNF #3100AO-102197) for grant support. We highly appreciate the technical and financial support of Philips Healthcare, Best, NL.

# *Figures*

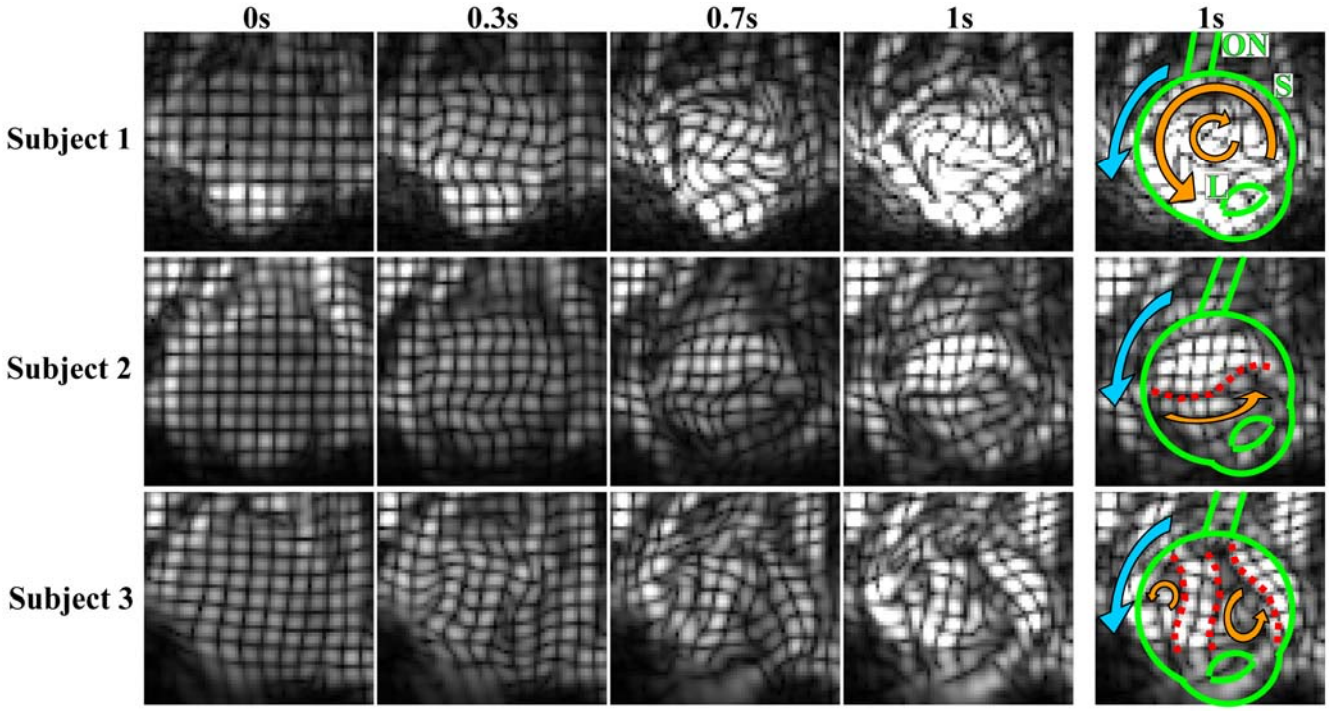


**Figure 1:** For three subjects, CSPAMM images of the right eye vitreous deformation during adduction are shown at the 1st, 5th, 10th, and 15th time frames. On the right, sketches illustrate the different vitreous deformation patterns of the three subjects. The blue arrows represent the eye movement direction; the yellow arrows indicate the local vitreous movement. The dotted red lines separate vitreous compartments with different viscoelasticity. The green lines indicate the optic nerve (ON), the sclera with the cornea (S), and the eye lens (L). Subject 1's vitreous has a homogeneous viscoelasticity and exhibits concentric deformation patterns around the rotation center. This type of deformation – found in 17 out of 19 Subjects – can be fitted by the analytical model. The vitreous of subjects 2 and 3 were polyphasic, i.e. divided – eventually by membranes (dotted lines) – into compartments of different viscoelastic properties. Some vitreous compartments do not or only slightly deform. In other compartments the eye movement induces the vitreous to whirl strongly and therefore the tagging pattern faded, making the deformation tracking impossible.

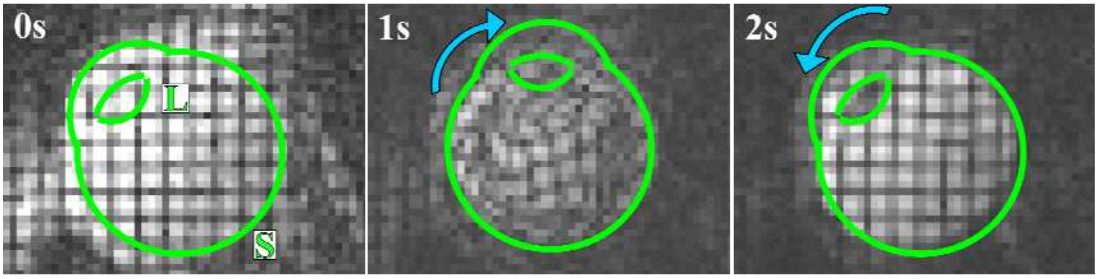


**Figure 2:** Axial CSPAMM images of a right eye vitreous deformation during a complete adduction-abduction-adduction cycle are shown at the 1st, 15th, and 30th time frames. The blue arrows represent the eye movement direction. The green lines indicate the sclera with the cornea (S), and the ocular lens (L). The vitreous of this subject has a homogeneous viscoelasticity and exhibits concentric deformation patterns around the rotation center. The eye movement induces the vitreous to whirl and therefore the tagging pattern to deform strongly. Nevertheless, this deformation is reversed by the eye's abduction, making the rectangular tagging pattern reappear at the 30th time frame. This proves that the whirling of the vitreous due to this type of sinusoidal eye movement remains in the laminar regime, as opposed to turbulent flow. The signal decrease of the eye lens due to its shorter T1 can also be observed.

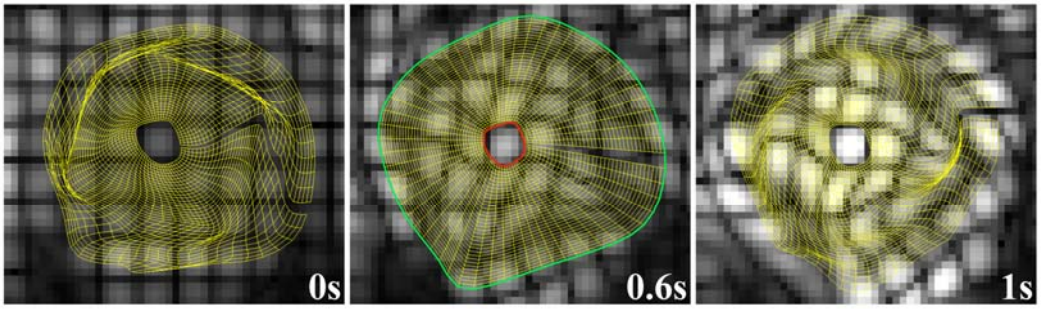


**Figure 3:** Axial CSPAMM image of the right eye vitreous during abduction-to-adduction at the 1st (0s), 9th (0.6s), 15th (1s) time frames. Superposed on the vitreous is the automatically tracked mesh (in yellow). At the 9th time frame, the red polygon was laid around the rotation center and had a radius slightly bigger than the tagline distance. The green polygon was laid on the border of the vitreous, i.e. on the sclera and the lens. The mesh was defined by radial interpolations of the red and green polygons. The mesh includes 36 concentric polygons of 60 vertices each. Each concentric polygon was tracked through the 15 time frames. The rotation of these concentric polygons is reported in function of time, in Fig4A. To better illustrate the mesh deformation, one segment of the concentric polygons has not been drawn.

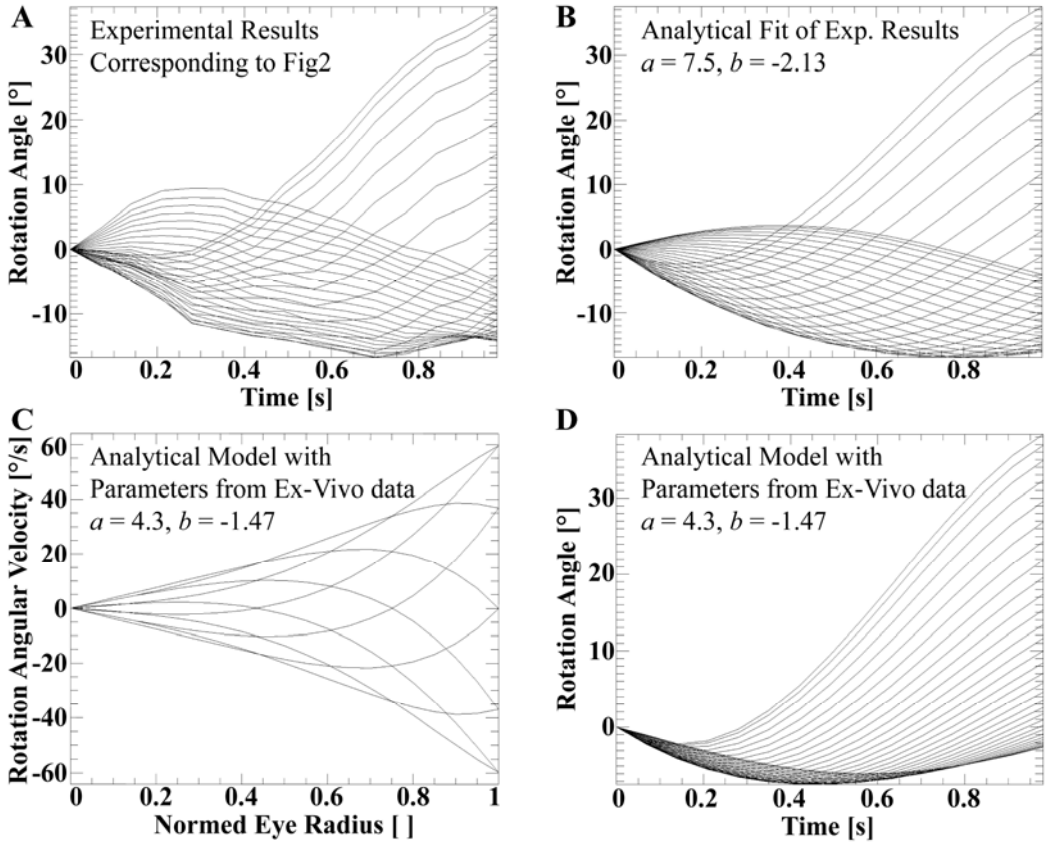


**Figure 4:** (**A**) Rotation angle as a function of time for each of the up to 36 concentric polygons of the mesh of Fig3. The outermost polygon undergoes a sinusoidal rotation of nearly 40°, corresponding to the gaze movement. The rotations of the other polygons differ in amplitude and phase. (**B**) Analytical model fitted to the vitreous deformation depicted in Panel A, determining *a* and *b*, from which the viscoelasticity can be calculated. (**C**) Deformation of the vitreous expected from a typical ex-vivo data set.(9,13) At r=0, the center of the eye ball, the circumferential velocity component represented here is (set to) zero due to symmetry, as the eye ball was assumed to be spherical. (**D**) From the radial velocity distribution for each time (see Fig7 in David, et al.(13)), the rotation angle over time of concentric circles was calculated for a better comparison with Panels (A) and (B).

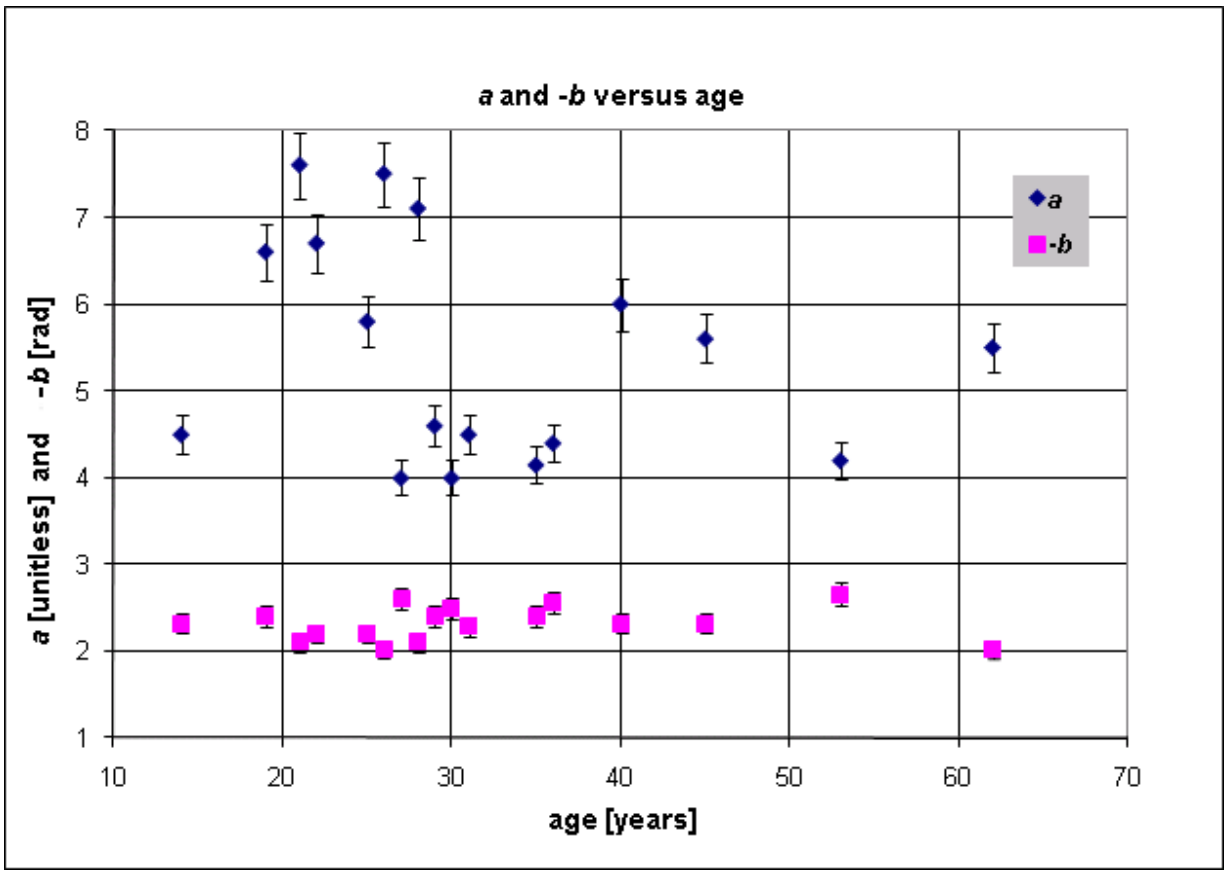


**Figure 5:** For each of the 17 subjects with monophasic vitreous, the *a* and -*b* values obtained from the fitting of the vitreous deformation with the analytical model are plotted as a function of the subject's age. The correlation coefficient between the age and *a* resp. *b* are -0.27 and 0.09, both not significant. The correlation coefficient between *a* and *b* is -0.76, significant with a double-sided f-test p-value smaller than 0.01. The drawn measurement error ranges on *a* and *b* are of 10%.

# References


1. Worst JGF, Los LI. Cisternal Anatomy of the Vitreous. Amsterdam: Kugler Publications; 1995. 150 p.
2. Forrester JV, Dick AD, McMenamin PG, Lee WR. The Vitreous. The Eye: Basic Sciences in Practice. Edition: 2, illustrated ed: Elsevier Health Sciences; 2002. p 204.
3. Stefansson E. Physiology of vitreous surgery. Graefe's archive for clinical and experimental ophthalmology = Albrecht von Graefes Archiv fur klinische und experimentelle Ophthalmologie 2009;247(2):147-163.
4. Neal RE, Bettelheim FA, Lin C, Winn KC, Garland DL, Zigler JS, Jr. Alterations in human vitreous humour following cataract extraction. Experimental Eye Research 2005;80(3):337-347.
5. Xu J, Heys JJ, Barocas VH, Randolph TW. Permeability and diffusion in vitreous humor: implications for drug delivery. Pharmaceutical Research 2000;17(6):664-669.
6. Gariano RF, Kim CH. Evaluation and management of suspected retinal detachment. American Family Physician 2004;69(7):1691-1698.
7. Nickerson CS, Park J, Kornfield JA, Karageozian H. Rheological properties of the vitreous and the role of hyaluronic acid. Journal of biomechanics 2008;41(9):1840-1846.
8. White HE, Levatin P. "Floaters" in the eye. Scientific American 1962;206:119-127.
9. Lee B, Litt M, Buchsbaum G. Rheology of the vitreous body. Part I: Viscoelasticity of human vitreous. Biorheology 1992;29(5-6):521-533.
10. Zimmerman RL. In vivo measurements of the viscoelasticity of the human vitreous humor. Biophysics Journal 1980;29(3):539-544.
11. Walton KA, Meyer CH, Harkrider CJ, Cox TA, Toth CA. Age-related changes in vitreous mobility as measured by video B scan ultrasound. Experimental Eye Research 2002;74(2):173-180.
12. Buchsbaum G, Sternklar M, Litt M, Grunwald JE, Riva CE. Dynamics of an oscillating viscoelastic sphere: a model of the vitreous humor of the eye. Biorheology 1984;21(1-2):285-296.
13. David T, Smye S, Dabbs T, James T. A model for the fluid motion of vitreous humour of the human eye during saccadic movement. Physics in medicine and biology 1998;43(6):1385-1399.
14. Repetto R. An analytical model of the dynamics of the liquefied vitreous induced by saccadic eye movements. Meccanica 2006;41:101-117.
15. Repetto R, Stocchino A, Cafferata C. Experimental investigation of vitreous humour motion within a human eye model. Physics in medicine and biology 2005;50(19):4729-4743.

16. Stocchino A, Repetto R, Cafferata C. Eye rotation induced dynamics of a Newtonian fluid within the vitreous cavity: the effect of the chamber shape. Physics in medicine and biology 2007;52(7):2021-2034.
17. Sebag J. To see the invisible: the quest of imaging vitreous. Developmental Ophthalmology 2008;42:5-28.
18. Litwiller DV, Pulido JS, Kruse SA, Glaser KJ, Ehman RL. MR Elastography of the Eye: Initial Feasibility Joint Annual Meeting ISMRM-ESMRMB. Berlin, Germany; 2007.
19. Li G, Zheng Y, Yang E. The feasibility of using MR elastography to measure stiffness of eye's muscle. 26th Annual Scientific Meeting of the ESMRMB. Antalya, Turkey; 2009.
20. Muthupillai R, Lomas DJ, Rossman PJ, Greenleaf JF, Manduca A, Ehman RL. Magnetic resonance elastography by direct visualization of propagating acoustic strain waves. Science 1995;269(5232):1854-1857.
21. Litwiller DV, Mariappan Y, Ehman RL. MR Elastography of the Ocular Vitreous Body. Joint Annual Meeting ISMRM-ESMRMB. Stockholm, Sweden; 2010.
22. Clayton EH, Wang Q, Song SK, Bayly PV. Non-invasive Measurement of Vitreous Humor Stiffness in the Mouse using MR Elastography. Joint Annual Meeting ISMRM-ESMRMB. Stockholm, Sweden; 2010.
23. Oyster CW. The Human Eye: Structure and Function. Sunderland, Mass.: Sinauer Associates; 1999. 795 p.
24. Dumars S, Andrews C, Chan WM, Engle EC, Demer JL. Magnetic resonance imaging of the endophenotype of a novel familial Mobius-like syndrome. Journal of AAPOS 2008;12(4):381-389.
25. Gonzalez RG, Cheng HM, Barnett P, Aguayo J, Glaser B, Rosen B, Burt CT, Brady T. Nuclear magnetic resonance imaging of the vitreous body. Science 1984;223(4634):399-400.
26. Piccirelli M, Luechinger R, Rutz AK, Boesiger P, Bergamin O. Extraocular muscle deformation assessed by motion-encoded MRI during eye movement in healthy subjects. Journal of vision 2007;7:14:5(14):1-10.
27. Fischer SE, Mckinnon GC, Maier SE, Boesiger P. Improved myocardial tagging contrast. Magnetic Resonance in Medicine 1993;30(2):191-200.
28. Piccirelli M, Luechinger R, Sturm V, Boesiger P, Landau K, Bergamin O. Local deformation of extraocular muscles during eye movement. Investigative Ophthalmology & Visual Science 2009;50(11):5189-5196.
29. Osman NF, Kerwin WS, McVeigh ER, Prince JL. Cardiac motion tracking using CINE harmonic phase (HARP) magnetic resonance imaging. Magnetic Resonance in Medicine 1999;42(6):1048-1060.

30. Ryf S, Tsao J, Schwitter J, Stuessi A, Boesiger P. Peak-combination HARP: A method to correct for phase errors in HARP. Journal of Magnetic Resonance Imaging 2004;20(5):874-880.
31. Kuijer JPA. Myocardial Deformation Measured with Magnetic Resonance Tagging [PhD Thesis]: Vrije Universiteit; 2000.
32. Gerthsen C, Kneser HO, Vogel H. Physik - Ein Lehrbuch zum Gebrauch neben Vorlesungen. 16 Auflage. Berlin: Springer-Verlag; 1992. p 144-148.
33. Busacca A. Biomicroscopie et Histopathologie de l'Oeil. Zürich; 1967. 25-43 p.
34. Eisner G. Clinical anatomy of the vitreous. In: Jacobiec FA, editor. Ocular Anatomy, Embryology, and Teratology. Philadelphia: Harper & Row Publishers; 1982. p 391-424.
35. Patz S, Bert RJ, Frederick E, Freddo TF. T(1) and T(2) measurements of the fine structures of the in vivo and enucleated human eye. Journal of Magnetic Resonance Imaging 2007;26(3):510-518.
36. Repetto R, Ghigo I, Seminara G, Ciurlo C. A simple hydro-elastic model of the dynamics of a vitreous membrane. Journal of Fluid Mechanics 2004;503:1–14.
37. Dr. Sherlock's Vitreous; DVD Supplement to the Goldmann-Lecture 2007. Eisner G. Heerbrugg: Swiss Ophthalmological Society; 2008.
38. Bishop PN. Structural macromolecules and supramolecular organisation of the vitreous gel. Progress in Retinal and Eye Research 2000;19(3):323-344.
39. Vappou J, Breton E, Choquet P, Goetz C, Willinger R, Constantinesco A. Magnetic resonance elastography compared with rotational rheometry for in vitro brain tissue viscoelasticity measurement. Magnetic Resonance Materials in Physics, Biology and Medicine 2007;20(5-6):273-278.
40. Bettelheim FA, Wang TJ. Dynamic viscoelastic properties of bovine vitreous. Experimental Eye Research 1976;23(4):435-441.
41. Kawano SI, Honda Y, Negi A. Effects of biological stimuli on the viscosity of the vitreous. Acta Ophthalmologica (Copenhagen) 1982;60(6):977-991.
42. Swindle KE, Hamilton PD, Ravi N. In situ formation of hydrogels as vitreous substitutes: Viscoelastic comparison to porcine vitreous. Journal of Biomedical Materials Research Part A 2008;87(3):656-665.
43. Gisladottir S, Loftsson T, Stefansson E. Diffusion characteristics of vitreous humour and saline solution follow the Stokes Einstein equation. Graefe's archive for clinical and experimental ophthalmology = Albrecht von Graefes Archiv fur klinische und experimentelle Ophthalmologie 2009;247(12):1677-1684.
44. Rutz A. Advances in Whole-Heart MRI Tagging for the Assessment of Myocardial Motion. Zurich: ETH Phd Thesis N° 17902; 2008.

45. Schovanec L. Ocular Dynamics and Skeletal Systems. IEEE control systems magazine 2001;21(4):70-79.
46. Zimmerman RA, Bilaniuk LT, Yanoff M, Schenck JF, Hart HR, Foster TH, Edelstein WA, Bottomley PA, Redington RW, Hardy CJ. Orbital magnetic resonance imaging. American journal of ophthalmology 1985;100(2):312-317.
47. Oyster CW. The Human Eye: Structure and Function. 1st edition ed. Sunderland, Mass.: Sinauer Associates; 1999. p 795, page 536.

# *Tables*

| | Elasticity $\varepsilon$ [$m^2/s$] | kinematic Viscosity $v$ [$m^2/s$] |
|---|---|---|
| minimum value | 0.026 | 0.050 |
| maximum value | 0.181 | 0.132 |
| average value | 0.093 | 0.089 |
| standard deviation | 0.053 | 0.028 |

**Table 1:** Vitreous viscosity $v$ and elasticity $\varepsilon$ calculated from the parameters $a$ and $b$ of the commonly used viscoelastic vitreous model best fitting the in-vivo vitreous deformation.